

# Bimodality of Freeman's Law

R. Brent Tully<sup>1</sup>, and Marc A.W. Verheijen<sup>2</sup>

<sup>1</sup> Institute for Astronomy, University of Hawaii  
2680 Woodlawn Drive, Honolulu, Hawaii 96822, USA

<sup>2</sup> Kapteyn Astronomical Institute  
Postbus 800, NL-9700 AV Groningen, The Netherlands

**Abstract.** A cluster sample of 62 galaxies complete to  $M_B = -16.5^m$  has been observed at  $B, R, I, K'$  bands with imaging detectors. The distribution of exponential disk central surface brightnesses is found to be bimodal. The bimodality is particularly significant at  $K'$  because obscuration is not a problem and because the high surface brightness galaxies are redder than the low surface brightness galaxies so the bifurcation is greater. The bimodality signal is especially clear when galaxies with close companions are excluded from consideration. High and low surface brightness pairs with essentially identical luminosities and maximum rotation characteristics are compared. It is suggested that the high surface brightness galaxies have self-gravitating disks while the low surface brightness galaxies are halo dominated at all radii. Evidently the intermediate surface brightness regime is unstable. If a disk has sufficiently low angular momentum and it shrinks enough that the disk potential begins to dominate the halo potential locally, then the disk must secularly evolve to the high surface brightness state characterized by a flat rotation curve.

## 1 Introduction

There has been a debate about whether the disks of galaxies have a quantized central surface brightness (Freeman 1970; van der Kruit 1987) or, instead, there is a broad distribution of disk central surface brightnesses (McGaugh, Bothun, and Schombert 1995; de Jong 1996). Disney (1976) and others have discussed the selection effects that could distort the observed surface brightness distribution. Surveys of the brightest galaxies tend to be dominated by the highest surface brightness objects. Special efforts are required to find low surface brightness galaxies (van den Bergh 1966; Impey, Bothun, and Malin 1988; Davies et al. 1994). It is difficult to have a proper normalization of the relative occurrence rates in different surface brightness intervals.

A large and complete sample of galaxies are considered in this study. The galaxies are drawn from the Ursa Major Cluster and the cluster assignment requires an appropriate redshift. The cluster is dynamically young (long crossing time, no central concentration, no ellipticals, many HI-rich spirals) and the galaxies may be representative of those in low density environments. There are 62 galaxies in the complete sample with  $M_B < -16.5^m$ . The data are presented in Tully et al. (1996).

CCD photometry at  $B, R, I$  bands has been acquired for all of the complete sample and  $K'$  HgCdTe images have been obtained for 60 of 62. This  $K'$  data

is a key to the discussion. First, the  $K'$  material is not affected significantly by obscuration so surface brightnesses are only modified by geometric effects associated with viewing perspectives. Second, higher surface brightness galaxies tend to be redder than lower surface brightness galaxies so the distinctions between the different classes that will be discussed are clearer as one progresses to the red.

## 2 Bimodality of Central Surface Brightnesses

There is a more complete presentation by Tully and Verheijen (1997), where the situation in all available passbands is discussed. Only the best evidence will be given here. The bimodality is found in all the observed bands but is the least ambiguous at  $K'$ . In addition, it turns out that the few intermediate surface brightness cases in our sample all have close companions. If the galaxies with substantial companions closer than 80 kpc in projection are excluded, the distribution of surface brightnesses of the remaining 36 of 60 galaxies with  $K'$  photometry is that seen in Figure 1.

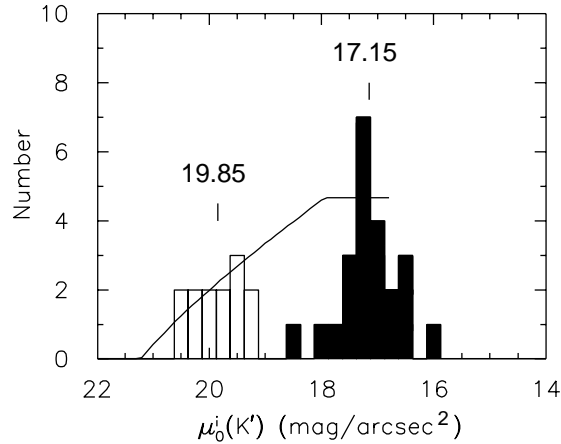


**Fig. 1.** Histogram of exponential disk central surface brightnesses at  $K'$ . Inclination corrected assuming no obscuration. Isolated galaxies only; galaxies with companions within 80 kpc projected are excluded. Filled histogram: HSB galaxies; open histogram: LSB galaxies. Solid curve: completeness expectation if there are equal numbers of galaxies in all surface brightness bins  $> 17$  mag/sq. arcsec. Means of the HSB and LSB distributions are indicated.

There is a clear separation into two peaks. The filled part of the histogram illustrates the  $K'$  equivalent of ‘Freeman’s law’. The galaxies that contribute belong to a *high surface brightness* [HSB] family. The open part of the histogram

is made up of constituents of a *low surface brightness* [LSB] family. The superimposed solid curve illustrates a completeness expectation assuming there is uniform population of the surface brightness–exponential scale length domain for scale lengths between 500 pc and 3 kpc and for all surface brightnesses faintward of 17 mag/sq. arcsec. It can be seen that the LSB peak has probably been reduced by incompleteness and may well have been truncated on the faint side. However, the critical point is that the visibility is quite adequate for the intermediate surface brightness regime between the HSB and LSB peaks and the paucity of objects in that region is highly significant.

### 3 Luminosity–Line Width and Surface Brightness–Scale Length Diagrams

Galaxies with essentially identical luminosities and rotation maxima can have very different central surface brightnesses and exponential scale lengths. These properties are demonstrated in Figure 2. The left panel shows the tight relation between  $K'$  luminosities and HI line profile widths. The line profiles have been transformed to approximate rotation maxima. HSB galaxies are represented by filled symbols and LSB galaxies, by open symbols. Three pairs are identified by numbers. The triplet identified by the letter *a* is two HSB galaxies, one with, and one without, a bulge and an LSB. The distinctions between bulge and non-bulge systems are discussed by Tully and Verheijen (1997).

The right panel illustrates the relation between  $K'$  central disk surface brightness and exponential scale lengths. Surface brightnesses have been corrected for inclination projection effects assuming no obscuration. Filled and open symbols have the same meaning as in the other panel. Crosses locate galaxies too faint to be in the complete sample. There are fewer data points in the left panel because only objects with satisfactory types, HI information, and inclinations could be plotted.

It is immediately seen how the HSB and LSB systems that were paired in the left panel have moved to separate domains in the right panel. Galaxies with a given total amount of light can be bright and compressed or dim and extended, yet generate the same rotation speeds. Galaxies apparently avoid an intermediate region in the parameter space of the right panel. The one-dimensional projection of the right panel of Fig. 2 onto the surface brightness axis gives the equivalent of Fig. 1 for the entire sample. The few intermediate surface brightness cases in Fig. 2 are filtered out of Fig. 1 because they are in close proximity to another galaxy.

### 4 Rotation Curve Disk–Halo Decompositions

Velocity field information will be made available for a large fraction of the Ursa Major sample (Verheijen 1997) but that work is still in progress. An HSB–LSB luminosity–rotation maximum pair that is not part of the Ursa Major sample has

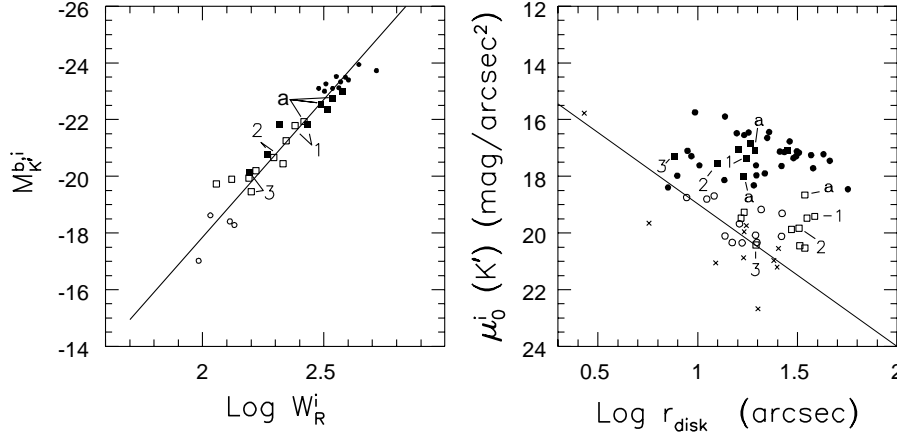


**Fig. 2.** *Left panel:* Luminosities at  $K'$  vs. HI profile line width; inclination corrected. Filled symbols: HSB; open symbols: LSB. HSB–LSB pairs with similar luminosities and linewidths are labeled 1,2,3. A bulge–nonbulge HSB pair and an LSB of comparable luminosity are labeled  $a$ . The solid line is the regression with uncertainties in line widths. *Right panel:*  $K'$  disk central surface brightness vs. exponential scale length. Symbols as in left panel with the addition that crosses are galaxies fainter than the completion limit. The same pairs and triplet are labeled. The solid line is the approximate completion limit.

been discussed in the literature. De Blok and McGaugh (1996) have decomposed the rotation curves of the HSB galaxy NGC 2403 and the LSB galaxy UGC 128. Their results are consistent with the following discussion.

At present, we consider only the three galaxies identified by the labels  $a$  in Fig. 2. One of these, NGC 3917, is an example of the LSB family. The other two are HSB examples: NGC 3949 has an exponential disk but no substantial bulge while UGC 6973 has a central concentration of light in addition to an exponential disk. Figure 3 provides a graphic summary of much of our information about these systems. There are  $B$  band images,  $I$  band surface brightness profiles, HI position-velocity maps, and rotation curve decompositions.

The rotation curve decompositions have three components. One is not important in any of these examples: the dotted curves indicate the contributions to rotational velocities from the interstellar gas. The dot-dash curves indicate the contributions due to the stellar distribution with an assumed fixed  $M/L$  value. The dashed curves are the residual contributions associated with a dark halo.

In each case, the same value of  $M/L_{K'} = 0.4M_{\odot}/L_{\odot}$  is assumed. This value is required for a ‘maximum disk’ fit (van Albada and Sancisi 1986) of the stellar components for the two HSB examples. Much larger  $M/L_{K'}$  values could be accommodated for the LSB case but still a dominant dark halo would be required. A parallel situation is found at  $B, R, I$ . It is expected that  $M/L$  values for LSBs would be lower, if anything, not higher than for the HSBs.

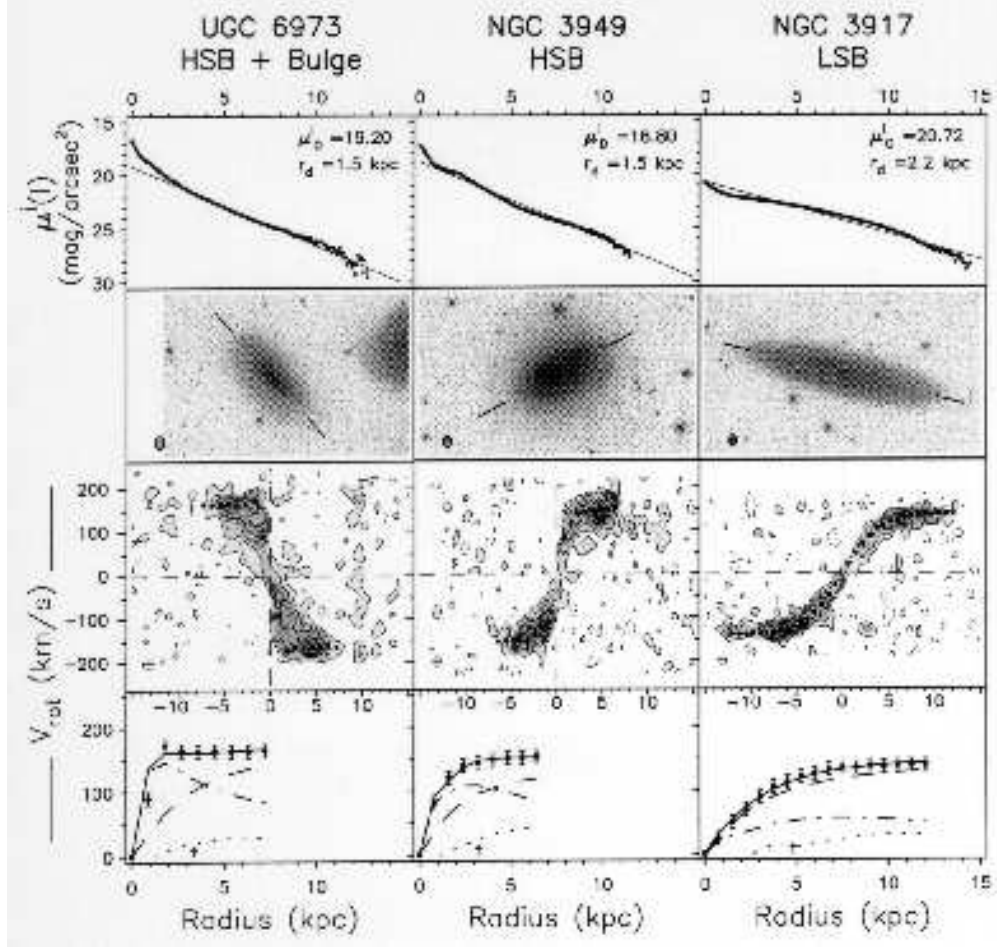


**Fig. 3.** Rotation curve decompositions. Examples of the three distinct classes of disk galaxies are presented in each of the vertical groups. On the left is UGC 6973, a system with a HSB exponential disk and a central bulge. In the middle is NGC 3949, a system with a HSB disk but no appreciable bulge. On the right is NGC 3917, a system with a LSB disk and no bulge. In each case, the horizontal axes are position in kpc. In the top and bottom panels the origin with respect to the nucleus is at the left axis, while in the middle panels the origin with respect to the nucleus is at the center of the plots. Surface brightnesses at  $I$ , corrected for inclination, are shown in the top panels. Images at  $B$  are shown in the second row. The major axes are indicated, as well as the FWHM beam of the HI observations. The velocity-position decomposition of the HI observations is seen in the panels of the third row. Velocities averaged over annuli are given as dots. The rotation curve decompositions are provided in the bottom panels. The dots with error bars illustrate the observed rotation curves. Dot-dashed curves illustrate the amplitude of rotation expected from the observed distributions of light and  $M/L = 0.4$  at  $K'$ . The dotted curves illustrate the contribution expected from the gas component. The dashed curves demonstrate the contribution attributed to a dark matter halo modelled by an isothermal sphere. The solid lines indicate the sum of these three components.

In the LSB case, there is the same total luminosity as in the HSB cases, but the light is more diffuse. If  $M/L$  is fixed, then the mass associated with this light cannot generate such high velocities in the LSB galaxy. Yet comparable rotation velocities are observed in the LSB and HSB examples. For the HSB systems, reasonable masses associated with the observed light can explain the observed rotation in the inner regions. In the LSB case, the rotation cannot be explained by the stellar mass and must be associated with an invisible component.

Tully & Verheijen (1997) describe how a location in the  $\mu_0, r_d$  plane of the right panel of Fig. 2 maps into a specified ratio of the peak rotation velocity ascribed to the luminous disk,  $V_{max}^{disk}$ , to the maximum observed rotation velocity,  $W_R^i/2$ , assuming  $M/L = \text{constant}$ . Loci of constant values of  $V_{max}^{disk}/0.5W_R^i$  are almost horizontal lines in the right panel of Fig. 2. Hence the surface brightness histograms of Fig. 1 can be transformed into the histogram of this dynamical ratio shown in Figure 4.

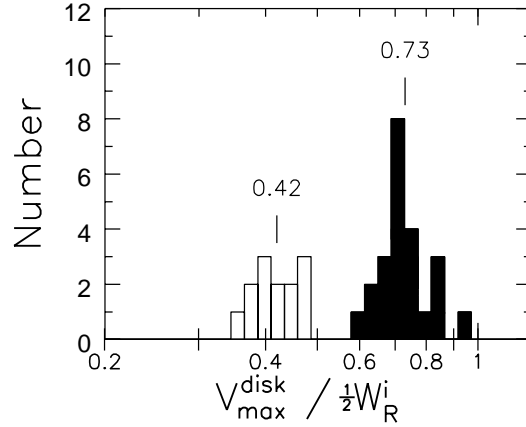


**Fig. 4.** Histogram of the ratio  $V_{max}^{disk}/0.5W_R^i$  based on photometric properties. Isolated sub-sample only (nearest important neighbor  $> 80$  kpc in projection). Values of  $V_{max}^{disk}$  follow from the properties of the exponential disk and  $M/L_{K'} = 0.4M_\odot/L_\odot$ . The relation between  $W_R^i$  and photometric parameters is given by the luminosity–line width correlation. Filled histogram: HSB systems; open histogram: LSB systems. Mean values for each family are indicated.

## 5 A Schematic Model

The speculation is offered that this difference between HSB and LSB systems is the rule. In LSB galaxies, the luminous material has settled into a disk that remains dominated by the halo potential. In HSB galaxies, the luminous material has become self-gravitating within the inner 2–3 scale lengths. Probably, the

difference is a question of angular momentum content or exchange. High angular momentum systems may come into rotational equilibrium in the LSB state. Low angular momentum systems, or parts of systems, may shrink until the disk becomes self-gravitating.

The speculation continues that once the disk becomes self-gravitating it must secularly evolve to find a stable configuration. Evidently, the intermediate surface brightness regime is disfavored. The gap is a factor of 10 in surface density. The stable regime seems to abide by the 'disk-halo conspiracy' (van Albada and Sancisi 1986) which produces a flat rotation curve. This situation is reminiscent of the arguments of Mestel (1963) for discrete states of radial stability.

## 6 Acknowledgements

Mike Pierce, Jia-Sheng Huang, and Richard Wainscoat participated in the collection of data. We thank Renzo Sancisi, Erwin de Blok, and Stacy McGaugh for constructive comments. This research has been supported by NATO Collaborative Research Grant 940271.

## References

- Davies, J.I., Disney, M.J., Phillipps, S., Boyle, B.J., Couch, W.J. 1994, *MNRAS*, **269**, 349.
- de Jong, R.S. 1996, *A&A*, **313**, 45.
- de Blok, W.J.G., McGaugh, S.S. 1996, *ApJL*, accepted.
- Disney, M.J. 1976, *Nat*, **263**, 573.
- Freeman, K.C. 1970, *ApJ*, **160**, 811.
- Impey, C.D., Bothun, G.D., Malin, D. 1988, *ApJ*, **330**, 634.
- McGaugh, S.S., Bothun, G.D., Schombert, J.M. 1995, *AJ*, **110**, 573.
- Mestel, L. 1963, *MNRAS*, **126**, 553.
- Tully, R.B., Verheijen, M.A.W., Pierce, M.J., Huang, J.S., Wainscoat, R.J. 1996, *AJ* **112**, 2471.
- Tully, R.B., Verheijen, M.A.W. 1997, *ApJ*, submitted.
- van Albada, T.S., Sancisi, R. 1986, *Phil. Trans. R. Soc. Lond. Ser. A*, **320**, 447.
- van den Bergh, S. 1966, *AJ*, **71**, 922.
- van der Kruit, P.C. 1987, *A&A*, **173**, 59.
- Verheijen, M.A.W. 1997, Ph.D. Thesis, University of Groningen, in preparation.